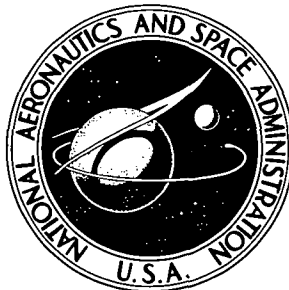


NASA TECHNICAL NOTE



N73-32627
NASA TN D-7406

NASA TN D-7406

CASE FILE
COPY

TECHNIQUE FOR PREDICTING
HIGH-FREQUENCY STABILITY CHARACTERISTICS
OF GASEOUS-PROPELLANT COMBUSTORS

by Richard J. Priem and Jefferson Y. S. Yang

Lewis Research Center

Cleveland, Ohio 44135

1. Report No. NASA TN D-7406	2. Government Accession No.	3. Recipient's Catalog No.	
4. Title and Subtitle TECHNIQUE FOR PREDICTING HIGH-FREQUENCY STABILITY CHARACTERISTICS OF GASEOUS-PROPELLANT COMBUSTORS		5. Report Date October 1973	6. Performing Organization Code
		8. Performing Organization Report No. E-7473	10. Work Unit No. 502-04
7. Author(s) Richard J. Priem and Jefferson Y. S. Yang		11. Contract or Grant No.	
		13. Type of Report and Period Covered Technical Note	
9. Performing Organization Name and Address Lewis Research Center National Aeronautics and Space Administration Cleveland, Ohio 44135		14. Sponsoring Agency Code	
		12. Sponsoring Agency Name and Address National Aeronautics and Space Administration Washington, D. C. 20546	
15. Supplementary Notes			
16. Abstract A technique for predicting the stability characteristics of a gaseous-propellant rocket combustion system is developed based on a model that assumes coupling between the flow through the injector and the oscillating chamber pressure. The theoretical model uses a lumped parameter approach for the flow elements in the injection system plus wave dynamics in the combustion chamber. The injector flow oscillations are coupled to the chamber pressure oscillations with a delay time. Frequency and decay (or growth) rates are calculated for various combustor design and operating parameters to demonstrate the influence of various parameters on stability. Changes in oxidizer design parameters had a much larger influence on stability than a similar change in fuel parameters. A complete description of the computer program used to make these calculations is given in an appendix.			
17. Key Words (Suggested by Author(s)) Combustion stability Gaseous propellant combustors Theoretical model		18. Distribution Statement Unclassified - unlimited	
19. Security Classif. (of this report) Unclassified	20. Security Classif. (of this page) Unclassified	21. No. of Pages 39	22. Price* Domestic, \$3.00 Foreign, \$5.50

TECHNIQUE FOR PREDICTING HIGH-FREQUENCY STABILITY CHARACTERISTICS OF GASEOUS-PROPELLANT COMBUSTORS

by Richard J. Priem and Jefferson Y. S. Yang*

Lewis Research Center

SUMMARY

A technique for predicting the stability characteristics of gaseous-propellant combustors is developed based on a model which assumes that the system is driven by coupling between the flow through the injector and the oscillating chamber pressure. The theoretical model uses a lumped parameter approach for the flow elements in the injection system plus wave dynamics in the combustion chamber. Stability characteristics (frequency and decay or growth rates) were calculated for various combustor design and operating conditions to demonstrate the influence of various parameters on stability. These results show that the stability of a given combustor is determined by the oxidant to fuel mixture ratio and that design changes in the oxidizer side of the system have a much larger influence on stability than similar changes in the fuel system.

INTRODUCTION

Recent interest by NASA in using hydrogen-oxygen thrusters for the Space Shuttle attitude control propulsion system (ACPS) has resulted in an extensive technology program. In this program (ref. 1) the gas/gas feed system received the greatest amount of attention and technology effort. The gas/gas feed system offers the advantages of versatility, flexibility, and light weight and the ability to be developed into a reliable high performance, fully reusable system with excellent thruster pulsing performance (ref. 2). To achieve the desired reliability and reusability will require that the system be designed, tested, and proven to have the same "dynamic" stability required for the Space Shuttle main engines (SSME) in the Space Shuttle Orbiter (ref. 3).

* Summer Faculty Fellow at the Lewis Research Center in 1971 and 1972; Assistant Professor of Engineering, Pacific Lutheran University, Tacoma, Washington.

For liquid/liquid and gas/liquid feed systems, as used in the SSME, several analytical models (refs. 4 to 7) are available for predicting combustor stability characteristics. These models have been used extensively in engine development programs to ensure that preliminary designs had the desired stability. The object of the program reported herein is to provide an analytical model for gas/gas rockets to predict stability characteristics. The analytical model of reference 6 predicts that gaseous flow variations through the injector are responsible for many of the stability characteristics observed in gas/liquid injectors. Therefore, this model was used as the basis for an all gaseous-propellant system.

The lumped-element model (ref. 6) for the dynamic flow characteristics of the gaseous injector was used in this investigation. Since dynamic stability (ability to damp a high amplitude disturbance in a finite period of time) would be required of any engine using gas/gas injection, the technique of solving for a neutral stability design point as used in references 5 to 6 was not considered adequate. Therefore, the analytical model was set up to calculate the frequency and decay rate (or growth rate if the engine is inherently unstable) for a specific combustor design and operating condition. This allows the designer to calculate the decay rate for his combustor to ensure that it meets the requirements for a "dynamically" stable engine.

After the analytical model was developed it was used to calculate the stability characteristics of a "standard" engine that might be used to meet the requirements for an ACPS thruster. Calculations were also performed for various perturbations of combustor design and operating parameters to demonstrate the usefulness of the model and the sensitivity of the stability characteristics to these parameters. To enable others to use the analytical model a complete listing of the computer program used to make the calculations, along with a description of the input and output and a sample calculation, is presented in the appendixes.

SYMBOLS

A_o	injector orifice area
A_t	nozzle throat area
a	chamber speed of sound
B_1, B_2	eqs. 15(a) and (b)
C	characterizes mass "capacitance time" of injector dome (eq. 10(a))
C_d	injector orifice coefficient
C^*	nozzle throat choked speed of sound

G_N	nozzle acoustic admittance, see eq. (16)
g	gravitational constant
I	characterizes flow "inductance" of injector duct (eq. 10(c))
J_n	n^{th} order Bessel function
K	eq. (17)
L	length
l	longitudinal wave mode number, $l = 0, 1, 2, \text{ etc.}$
M	chamber Mach number
M_w	molecular weight
m, n	transverse wave mode numbers, $m = 1.84, 5.33, 8.53, \text{ etc.}$ for $n = 1$; $m = 3.05, 6.70, \text{ etc.}$ for $n = 2$
N_b	propellant burning response, see eq. (19)
N_c	chamber flow response, see eq. (18)
N_{inj}	injector flow response, see eq. (9)
O/F	oxidizer to fuel flow ratio
P	pressure
P_{choke}	dome pressure for choked flow as defined in eq. (3)
R	characterizes flow "conductance" of injector orifice (eq. 10(b))
R_c	chamber radius
R_o	universal gas constant
r	chamber radial direction
s	complex frequency, $\alpha + i\omega$
T	total temperature of propellant
t	time
V_d	dome volume of propellant
V_z	chamber axial velocity
W	mass flow rate of propellant
W_N	mass flow rate through nozzle
W_t	total mass flow rate
z	chamber axial direction

α	oscillation growth rate or decay rate if negative
γ	ratio of specific heats
η_{C^*}	C^* efficiency
θ	chamber tangential direction
ρ	density
τ	delay time
ω	angular frequency
ω_0	natural frequency

Subscripts:

d	dome
c	chamber
o	orifice

Superscripts:

—	mean
'	perturbed, $X - \bar{X}$

THEORY

The analytical model treats the rocket as a system consisting of the injector, combustion chamber, and a combustion region with the appropriate boundary and compatibility conditions at the interface of the various regions. The flow in each region responds to an impressed acoustic pressure oscillation originating in the combustion chamber. These flow responses are influenced by the geometrical and gas dynamic conditions in the injector and combustion chamber. All dependent variables are written as the sum of a constant mean term and a small magnitude term that is harmonic in time. All governing equations are thereby linearized by this small perturbation technique.

Injector

The flow response in the injector is based on the analysis of Feiler and Heidmann (ref. 6) with modifications to include compressible flow through the injector orifices. A schematic of the injector with its various elements is shown in figure 1. All the dimensions of the various elements in the injector are considered to be small compared to the

wavelength of the oscillations. This permits a lumped-parameter treatment of the various elements in the injector.

Propellant Supply Line and Dome

A continuous flow of propellant to the supply dome is assumed. Since the flow is compressible and isentropic, pressure oscillations will affect the instantaneous total mass in the dome so that the dome acts as a capacitor for the flow. Perturbing the dome total mass balance, we get

$$\frac{\bar{\rho}_d V_d}{\gamma \bar{P}_d} s P_d' = -W' \quad (1)$$

The dome mean pressure \bar{P}_d is determined by combining the mean pressure drop across the injector orifice with the mean chamber pressure:

$$\bar{W} = A_o C_d \bar{P}_d \sqrt{\frac{2\gamma}{\gamma - 1} \frac{M_w}{R_o \bar{T}} \left[\left(\frac{\bar{P}_o}{\bar{P}_d} \right)^{2/\gamma} - \left(\frac{\bar{P}_o}{\bar{P}_d} \right)^{(\gamma+1)/\gamma} \right]} \quad (2)$$

and \bar{P}_d is solved using a curve-fitting technique and $\bar{P}_o = \bar{P}_c$.

For certain chamber pressures and propellant flow rates the flow may become choked. The dome pressure for choked flow is then given by

$$\bar{P}_{\text{choke}} = \frac{\bar{P}_c}{\left(\frac{2}{\gamma + 1} \right)^{\gamma/\gamma-1}} \quad (3)$$

If the flow is actually choked for the given flow rate \bar{W} , the dome pressure is given by

$$\bar{P}_d = \frac{\bar{W}}{A_o C_d \sqrt{\frac{2\gamma}{\gamma - 1} \frac{M_w}{R_o \bar{T}} \left(\frac{\bar{P}_c}{\bar{P}_{\text{choke}}} \right)^{2/\gamma} - \left(\frac{\bar{P}_c}{\bar{P}_{\text{choke}}} \right)^{(\gamma+1)/\gamma}}} \quad (4)$$

The dome gas density is described by the perfect gas equation

$$\bar{\rho}_d = \frac{\bar{P}_d}{R_o \bar{T} / M_w} \quad (5)$$

Injector Flow Duct and Orifice

With a short length duct the flow can be assumed incompressible with uniform mean pressure within the duct. The perturbed momentum equation is used to obtain the pressure drop across the duct:

$$P'_o - P'_c = \frac{L_o}{A_o g} s W' \quad (6)$$

To obtain the flow perturbation through the injector produced by the pressure perturbations on either side of the orifice the compressible orifice flow equation (2) is perturbed to obtain

$$\left\{ \frac{1}{\gamma} - \frac{\frac{\gamma-1}{2\gamma}}{\bar{P}_c^{(1-\gamma)/\gamma} [\bar{P}_d^{(\gamma-1)/\gamma} - \bar{P}_c^{(\gamma-1)/\gamma}]} \right\} \frac{P'_o}{\bar{P}_c} + \left\{ \frac{\frac{\gamma-1}{2\gamma}}{\bar{P}_d^{(1-\gamma)/\gamma} [\bar{P}_d^{(\gamma-1)/\gamma} - \bar{P}_c^{(\gamma-1)/\gamma}]} \right\} \frac{P'_d}{\bar{P}_d} = \frac{w'}{\bar{W}} \quad (7)$$

Injector Flow Response

The flow oscillation of the injector system is a function of the pressure oscillation in the combustion chamber. This function is expressed as an admittance as given by

$$N_{inj} = \frac{W'/\bar{W}}{P_c/P_c} \Big|_{\text{injector exit}} \quad (8)$$

Substitution of equations (1), (6), and (7) into equation (8) gives

$$N_{inj} = - \frac{Cs}{1 + CRs + CIs^2} \quad (9)$$

$$C = - \frac{\bar{p}_d V_d}{\gamma \bar{W}} \left\{ \frac{\frac{1}{\gamma} + \frac{\gamma - 1}{2\gamma} \left[\frac{1}{1 - \bar{P}_c^{(1-\gamma)/\gamma} \bar{P}_d^{(\gamma-1)/\gamma}} \right]}{\frac{\gamma - 1}{2\gamma} \left[\frac{1}{1 - \bar{P}_c^{(\gamma-1)/\gamma} \bar{P}_d^{(1-\gamma)/\gamma}} \right]} \right\} \quad (10a)$$

$$R = - \frac{1}{\frac{1}{\gamma} + \frac{\gamma - 1}{2\gamma} \left[\frac{1}{1 - \bar{P}_c^{(1-\gamma)/\gamma} \bar{P}_d^{(\gamma-1)/\gamma}} \right]} \quad (10b)$$

$$I = \frac{\bar{W} L_o}{\bar{P}_c A_o g} \quad (10c)$$

The real part of N_{inj} indicates the degree to which the flow responds in phase with the impressed pressure oscillation. The imaginary part of N_{inj} indicates the amount of flow oscillation out of phase with the impressed pressure oscillation.

Combustor Chamber

The mean flow in the combustion chamber is assumed to be uniform, one-dimensional, and inviscid. The gas in the combustion chamber is assumed to have the properties associated with the products of combustion for the mixture ratio being metered to the chamber. The gas properties (γ , M_w , and C^*) as functions of mixture ratio were obtained from the tables for hydrogen-oxygen propellants in reference 8. The mean chamber flow conditions were then calculated from the following:

Pressure:

$$\bar{P}_c = \frac{C^* W_t \eta C^*}{A_t g} \quad (11a)$$

Speed of sound:

$$a = \gamma C^* \sqrt{\left(\frac{2}{\gamma + 1} \right)^{(\gamma+1)/(\gamma-1)}} \quad (11b)$$

Density:

$$\bar{\rho}_c = \frac{\gamma \bar{P}_c g}{a^2} \quad (11c)$$

Mach number:

$$M = \frac{W_t}{\bar{\rho}_c a \pi R_c^2} \quad (11d)$$

The natural frequency of the chamber was calculated assuming hard walls as follows:

$$\omega_o = \frac{a}{R_c} \sqrt{m^2 + \left(\frac{\pi R_c l}{L_c}\right)^2} \quad (12)$$

The three-dimensional perturbed pressure and velocity fields in the chamber have previously been determined by Priem and Rice (ref. 9). With ω replaced by s/i ,

$$\frac{P'_c}{\bar{P}_c} = -\gamma \left[J_n(mr) e^{in\theta} e^{st} \right] \left[s \left(e^{B_1 z} + K e^{B_2 z} \right) + M \left(B_1 e^{B_1 z} + B_2 K e^{B_2 z} \right) \right] \quad (13)$$

$$\frac{v'_z}{a} = J_n(mr) e^{in\theta} e^{st} \left(B_1 e^{B_1 z} + B_2 K e^{B_2 z} \right) \quad (14)$$

where

$$B_1 = \frac{sM + \sqrt{(sM)^2 + (1 - M^2)(m^2 + s^2)}}{1 - M^2} \quad (15a)$$

$$B_2 = \frac{sM - \sqrt{(sM)^2 + (1 - M^2)(m^2 + s^2)}}{1 - M^2} \quad (15b)$$

and v'_z is the perturbed axial velocity. A constant K is determined from the boundary conditions as follows:

$$G_N = \left. \frac{W' \bar{P}}{\bar{W} P'} \right|_{\text{nozzle}} = \left(\frac{1}{\gamma} + \frac{v'_z}{M P'_c} \right)_{z=0} \quad (16)$$

then

$$K = - \frac{B_1 (1 - M^2 + \gamma G_N M^2) + sM(\gamma G_N - 1)}{B_2 (1 - M^2 + \gamma G_N M^2) + sM(\gamma G_N - 1)} \quad (17)$$

The flow perturbation response at the injector end of the chamber ($z = -L_c$) can then be written as

$$N_c = \left. \frac{W' \bar{P}}{\bar{W} P'} \right|_{\text{inj}} = \frac{1}{\gamma} - \frac{B_1 e^{-B_1 L_c} + B_2 K e^{-B_2 L_c}}{\gamma M^2 (B_1 e^{-B_1 L_c} + B_2 K e^{-B_2 L_c}) + \gamma sM (e^{-B_1 L_c} + K e^{-B_2 L_c})} \quad (18)$$

This flow perturbation response must be matched to the response produced by the injector-combustion process combination.

Combustion Process

The burning process which embodies the effects of propellant mixing and chemical reaction is assumed to be characterized by delay times τ for the fuel and oxidizer. It is also assumed that the burning process occurs in a very thin region (relative to the length of the chamber) immediately downstream of the injector.

The propellant burning response N_b is assumed to be the sum of the oxidizer and fuel response functions. The individual oxidizer and fuel responses are weighted by their fractional mass flow rates with a delay time to obtain the following:

$$N_b = \frac{1}{\bar{W}_t} \left(\bar{W}_{\text{inj}} e^{-\tau s} \right)_{\text{oxidizer}} + \frac{1}{\bar{W}_t} \left(\bar{W}_{\text{inj}} e^{-\tau s} \right)_{\text{fuel}} \quad (19)$$

Matching the propellant burning response function with the chamber response function produces the following boundary condition for the chamber-injector interface:

$$N_b - N_c = 0 \quad (20)$$

Equations (9) and (18) to (20) are solved together to obtain the chamber and injector flow responses along with the complex frequency. The imaginary part of the complex frequency describes the period of oscillation and the real part describes the damping rate. A positive value for the real part of the complex frequency means the system is spontaneously unstable and the oscillations will grow in amplitude with time.

Numerical Solution

The flow chart for the computer program to calculate stability is shown in figure 2. The program listing, the program input formats, and a sample calculation are given in appendixes A to C. The solution procedure is to first determine the mean chamber conditions and to test if the injector flows are choked. A guessed value of the complex frequency s is then used to initiate an iterative scheme to converge on a consistent s which satisfies the compatibility conditions of equation (20). The iterative process reduces the error between injector and chamber flow responses, which is the left side of equation (20), to zero by Taylor's formula for two variables.

For any given engine configuration and flow condition, there exist multiple solutions of the complex frequency s . These solutions can be determined from a table of flow response errors as functions of a range of s values. The lowest error values on the map will be at or near a solution. This point can be used as the assumed frequency to initiate the iterations or to check a solution. The quadrants on the complex plane in which the errors lie are also calculated as an additional check on the existence of a solution at the lowest point. A sample error map is tabulated in appendix C for frequencies between 51 000 and 90 000 radians per second and growth rates of 750 to -650 reciprocal seconds.

ANALYTICAL RESULTS

To examine the influence of injector and combustor parameters on stability, a base engine about which a parametric study could be performed was established. For the base engine it was assumed that the physical dimensions and mass flow rates would be representative of engines tested in the Space Shuttle attitude control propulsion system (ACPS) technology program. It was also assumed that the engine would have neutral stability (a disturbance would neither grow or decay) and that the oxidizer and fuel flow oscillations through the injector would be 180° out of phase with the chamber pressure oscillations. Furthermore, it was assumed that the ratio of the oxidizer to fuel flow oscillation was the same as the ratio of the oxygen to fuel flow rate. It was also assumed that the delay times of the fuel and oxidizer corresponded to a half period of the oscillations.

TABLE I. - STANDARD ENGINE

(a) Combustion chamber

Length, L_c , ft	0.5
Radius, R_c , ft	0.1575
Nozzle throat area, A_t , ft^2	0.0185
Nozzle throat choked speed of sound efficiency, η_{c*}	1.0
Nozzle admittance, G_n	$0.9166 + 0.0 i$
Pressure wave numbers:	
For $n = 0$	0
For $m = 1.84$	1
For $l = 0$	0
Standard growth rate, α , 1/sec	0.0
Standard angular frequency, ω , Hz	9950
Standard chamber response, N_c	$0.9174 + 0.0 i$

(b) Injector

	Oxidizer	Fuel
Dome volume, V_d , ft^3	0.0036574	0.0024363
Orifice length, L_o , ft	0.00027833	0.0098092
Orifice area, A_o , ft^2	0.0019514	0.0030957
Orifice coefficient, C_d	1.0	1.0
Mass flow rate, W , lb/sec	2.658	0.505
Specific heat ratio, γ	1.36	1.41
Temperature per molecular weight, T/M_w , $^{\circ}R/lb$	16.875	393.0
Combustion delay time, τ , sec	0.000050255	0.000050255

The physical and gas dynamical properties of the standard engine are shown in table I. Additional information on the standard engine can be found in the sample calculation in appendix C.

Stability Characteristics of Standard Engine

The stability of the standard engine operating at various fuel and oxidizer flow rates is shown in figure 3(a). The lines of constant growth rates (α/ω , fraction/cycle) originate at the origin of the plot and correspond to constant values of O/F (oxidant flow rate/fuel flow rate). Examining the equations that are used in the solutions reveals that flow rates can be eliminated in the equations by dividing by total flow rate and converting the equations to O/F. Therefore, the engine O/F uniquely defines the stability of an engine, independent of flow rates, for fixed values of the other parameters.

Stability of the standard engine as a function of O/F is shown in figure 3(b). At very low and high mixture ratios the engine is stable. Between a mixture ratio of 0.35 and 5.26 the engine is unstable. A growth rate of 0.1 fraction per cycle is very unstable as an oscillation with an amplitude of 1 percent of chamber pressure would grow to an amplitude of 100 percent in 48 cycles or 5 milliseconds.

At the very low O/F the fuel side of the injector is operating in the choked flow regime. Therefore, it does not respond to the pressure oscillations. The oxidizer side of the injector is operating at a very low injector pressure drop to chamber pressure ratio, which results in a large flow response, but the fraction of total propellant flow that is being oscillated is small so the engine is stable. At the high O/F ratio the opposite is true with the oxidizer flow being choked and the fuel only being a small fraction of the total flow. In the intermediate O/F region both the fuel and oxidizer respond to a pressure oscillation with sufficient magnitude to make the engine unstable.

Influence of Design Parameters on Stability

To demonstrate the effect of the various design variables on stability, calculations to determine the growth or decay rate of the first transverse mode ($n = 1$, $m = 1.84$, and $l = 0$) were made in which each design variable was individually increased and decreased about the value it had in the standard engine. The results are plotted in terms of growth rate as a function of the oxidant to fuel flow ratio (O/F) in figure 4. The range of each variable was arbitrarily selected to represent a reasonable range over which the design might be changed.

The influence of the chamber radius and nozzle throat area is shown in figures 4(a) and (b). Increasing either the chamber radius or throat area significantly improved stability (curves are lower and less area under the curves). The reasons for the improved stability with these two variables are entirely different. The change in chamber radius changed the frequency of the oscillation with a resultant detuning of the system. A nozzle throat area increase decreased the chamber pressure and as a result increased the ratio of injector pressure drop to chamber pressure, thereby decoupling the injector flow from the chamber pressure oscillations.

The influence of changes in oxidizer injector length, dome volume, and orifice area on stability is shown in figures 4(c), (e), and (g). The stability at high O/F ratios was not influenced by changing any of the oxidizer variables. This is because at high O/F's the oxidizer flow is choked and, therefore, does not respond to any pressure oscillations; therefore, the oxidizer variables are not important in stability under these conditions. Increasing the oxidizer injector length to 0.03 feet made the engine stable over the entire mixture ratio. This is because the high inertial effect of a long orifice prevents the oxygen flow from responding to a pressure oscillation. Decreasing the oxidizer orifice

area had a similar effect. Decreasing the oxidizer dome volume improved stability by reducing the reservoir that stores the propellant when the flow oscillates.

The influence of changes in the fuel variables are shown in figures 4(d), (f), and (h). The fuel variables did not influence stability at the low O/F ratios because in this region the fuel flow is choked and does not respond to any pressure oscillations; thus, the fuel variables are not important under these conditions. At high O/F ratios the fuel side variables influenced stability in a manner similar to that described previously for the oxidizer side; however, the influence of the fuel variables on stability was much less than that observed with the oxidizer variables.

Increasing the fuel and oxidizer flow properties (ratio of temperature to molecular weight) improved stability in a manner similar to those described previously for the injector (figs. 4(i) and (j)). Fuel properties had no influence on stability at the low O/F's, and the oxidizer had no influence at high O/F's. Increasing the temperature over molecular weight ratio improved stability by increasing the injector pressure drop, thereby decreasing the flow oscillations that could be produced by a given pressure oscillation. Again, changing the oxidant properties produced a larger influence on stability than did the fuel property changes.

The influence of the oxidizer and fuel delay times on stability is shown in figures 4(k) and (l). Decreasing the oxidizer delay time to 3×10^{-5} second (corresponding to burning in 0.3 in.) produced a very stable engine over the entire O/F region. Increasing the oxidizer delay time produced a stable operating region from an O/F of 0.8 to 5. Again, a change in oxidizer delay time did not influence stability at the high O/F ratios. Changing the fuel delay time had a similar influence on stability as the oxidizer delay time but produced a much smaller change in stability.

Looking at all the parameters together we see that the standard engine could be made very stable by increasing the chamber radius, throat area, oxidizer injector length, or reducing the oxidizer orifice area and delay time. Of these, the changes in throat area and orifice area influence the supply pressure and chamber pressure which might not be satisfactory from the overall systems point of view. Stability, therefore, would be easiest to obtain in this engine by increasing the oxidizer orifice length to 0.05 feet (0.6 in.) and decreasing the delay time by a factor of 2 to 0.00025 second.

SUMMARY OF RESULTS

A technique for predicting the stability characteristics of gaseous propellant combustors has been developed based on a model which assumes that the system is driven by coupling between the flow through the injector and chamber pressure oscillations. The technique was used to calculate the influence of various combustor design and operating

parameters on stability. The results of these calculations may be summarized as follows:

1. The stability of a given combustor was determined by the oxidant to fuel mixture ratio for any fuel or oxidant flow rate.
2. Changing design parameters in the oxidizer side of the injector influences the stability characteristics at low oxidant to fuel mixture ratios, while changes in the fuel system influenced the stability characteristics at high oxidant to fuel mixture ratios.
3. Changes in the design of the oxidizer system had a much larger influence on stability than a similar change in the fuel system.
4. Changing the chamber radius or nozzle throat also had a large effect on the stability of a combustor.
5. To obtain maximum stability in a combustor with given propellant flow rates the combustor should have a large chamber radius and throat area. The injector oxidizer orifices should have a small total area, a long length, and should produce a very small delay time between when the oxidizer is injected and burned.

Lewis Research Center,

National Aeronautics and Space Administration,

Cleveland, Ohio, June 25, 1973,

502-04.

APPENDIX A

COMPUTER LISTINGS

\$IBFTC MAIN

```
REAL LL, MW, LOX, LF, IOX, IFU, MACH, NBR, NBI, NCR, NCI
COMPLEX CSROX, CSRF, ISOX, ISF, TAUSOX, TAUSF
COMPLEX NC(3), SZ, SZHZ, GNOZ, SS, SSAVE
COMPLEX S(3), NB(3), NBOX, NBF, ERR(3), ESAVE1, ESAVE2
INTEGER WHICH, FRCUT, FICUT, REGION
DIMENSION EI(3), ER(3)
DIMENSION F(200), T(15)
DIMENSION Z1(26), Z2(26), IZ1(26), IZ2(26), Z3(26), Z4(26), IZ3(26)
COMMON/BF/F
COMMON/ERM/FRMAX, FIMAX, FRMIN, FIMIN, FRCUT, FICUT, IOX, ROX, COX,
*TAUOX, CFU, RFU, IFU, TAUF, IFLAGO, IFLAGF, WF, WOX
COMMON/WH/ R, AT, TOMOX, TOMF, AOX, AF, LOX, LF, VOX, VF
COMMON /SCLL/VZ, AMOR, AMV, GC, VV, LL, AA, GNR, GNI
COMMON /AMAIN/PI, GCON, GASC, PC, WTOT
READ (5,150) WMAX, WMIN, GAMOX, CORFOX, AOX, LOX
READ (5,149) VOX, TAUOX, TOMOX, IP, DELX
READ (5,150) WFMAX, WFMIN, GAMF, CORFF, AF, LF
READ (5,149) VF, TAUF, TOMF, MAP
READ (5,151) LL, R, AT, CSTREF, GNR, GNI, SM, SL
READ (5,174) WOSTD, WFSTD, DW, DWF
IF (IP.EQ.0) READ (5,175) FRINP, FIINP, INPUTF
IF (IP.NE.0) READ (5,174) (Z1(I), Z2(I), Z3(I), Z4(I), IZ1(I),
*IZ2(I), IZ3(I), I=1, IP)
IF (MAP.NE.0) READ (5,174) FRMAX, FRMIN, FIMAX, FIMIN, FRCUT, FICUT
IF (IP.NE.0) GO TO 1040
IP=1
Z3(1)=FRINP
Z4(1)=FIINP
IZ1(1)=0
IZ3(1)=1
1040 DO 1000 MN=1, IP
IM=MN-1
IF (MN.EQ.1) IM=1
CALL RSTRP (MN, IZ1 (IM))
1001 PMAX=Z1 (MN)
PMIN=Z2 (MN)
FRINP=Z3 (MN)
FIINP=Z4 (MN)
WHICH=IZ1 (MN)
NP=IZ2 (MN)
INPUTF=IZ3 (MN)
GNOZ=CMLPX (GNR, GNI)
WRITE (6,152)
WRITE (6,171)
WRITE (6,153)
WRITE (6,154)
WRITE (6,155) WMAX, WMIN, GAMOX, CORFOX, AOX, LOX, VOX, TAUOX, TOMOX, DW,
*WOSTD
WRITE (6,156)
WRITE (6,154)
WRITE (6,155) WFMAX, WFMIN, GAMF, CORFF, AF, LF, VF, TAUF, TOMF, DWF, WFSTD
```

```

WRITE(6,157)
WRITE(6,158)
WRITE(6,155) LL,R,AT,CSTREF,SM,SL,GNOZ,IP
WRITE(6,710)
WRITE(6,155) DELX,PMAX,PMIN,WHICH,NP,MAP
WRITE(6,730)
WRITE(6,155)FRINP,FIINP,INPUTF
FIINP=FIINP*2.*PI
WRITE(6,172)
DP=0.
IF(NP.EQ.1) GO TO 401
DP=(PMAX-PMIN)/FLOAT(NP-1)
401 DO 500 JP=1,NP
REGION=0
IF(WHICH.EQ.0) GO TO 440
CALL WHICHP(WHICH,JP,PMAX,DP)
440 REGION=REGION+1
WOX=WOSTD
GO TO (400,410,410,400), REGION
400 NO=IFIX(ABS(WOSTD-WMIN)/DW)+1
GO TO 415
410 NO=IFIX(ABS(WOSTD-WMAX)/DW)+1
415 IF(REGION.LE.2) GO TO 3
NO=NO-1
WOX=WOSTD-DW
IF(REGION.EQ.3) WOX=WOSTD+DW
3 DO 70 M=1,NO
GO TO (420,430,420,430),REGION
420 NF=IFIX(ABS(WFSTD-WFMAX)/DWF)+1
GO TO 250
430 NF=IFIX(ABS(WFSTD-WFMAX)/DWF)+1
250 WF=WFSTD
IF(REGION.EQ.1.OR.REGION.EQ.3) GO TO 311
NF=NF-1
WF=WFSTD-DWF
311 DO 60 I=1,NF
COX=1.
CFU=1.
L=1
WTOT= WOX+WF
OF=WOX/WF
FRACT= 1./(OF+1.)
CALL CHMBR(FRACT,CSTR,GC,MW)
PC= CSTR*WTOT/(AT*GCON)*CSTREF
PCSI=PC/144.
B= (GC+1.)/(GC-1.)
A= GC*SQRT((2./(GC+1.))**B)*CSTR
FG= A*SQRT(SM**2.+(SL*PI*R/LL)**2.)/R
FREQN=FG/(2.*PI)
ALFAZ=0.
FREQZ=FG
S(1)= CMPLX(0.,FG)

```

```

IF (INPUTF.EQ.1) S(1)=CMPLX(FRINP,FIINP)
IF (JP.GT.1.OR.I.GT.1) S(1)=SZ
IF (M.GT.1.AND.I.EQ.1) S(1)=SSAVE
ALFG=REAL(S(1))
FG=AIMAG(S(1))
AA=A*A
RHOC=GC*PC*GCON/AA
VZ=WTOT/(PI*RHOC*R**2.)
VOA=VZ/A
VV=VZ*VZ
AMV=AA-VV
AMOR=AA*(SM/R)**2.
MACH=VV/AA
CALL WOP(GAMOX,CORFOX,WOX,AOX,TOMOX,VOX,LOX,COX,ROX,IOX,RHOX,
*DELPO,IFLAGO,PCHOKO)
DELPOX=DELPO/144.
PDOX=(PC+DELPO)/144.
DPOPCO=DELPO/PC
7 CALL WOP(GAMF,CORFF,WF,AF,TOMF,VF,LF,CFU,RFU,IFU,RHOF,DELPFU,
*IFLAGF,PCHOKF)
DELPF=DELPFU/144.
PDF=(PC+DELPFU)/144.
DPOPCF=DELPFU/PC
IF (MAP.EQ.1.AND.IM.EQ.1) CALL ERMAP
IM=0
1 DF=DELX*FG*MACH
DA=DELX*.1*ALFG
DAA=10.*DELX
IF (DAA.GT.DA) DA=DAA
DO 10 J=1,3
NBOX=0.
NBF=0.
IF (IFLAGO.EQ.1) GO TO 4
CALL NBS(IOX,ROX,COX,TAUOX,S(J),NBOX,VCTROX,THETAO)
4 IF (IFLAGF.EQ.1) GO TO 8
CALL NBS(IFU,RFU,CFU,TAUF,S(J),NBF,VCTRF,THETAF)
8 NB(J)=(WOX*NBOX+WF*NBF)/WTOT
CALL NCS(S(J),NC(J))
ERR(J)=NB(J)-NC(J)
IF (CABS(ERR(J)).LE..01) GO TO 50
ER(J)=REAL(ERR(J))
EI(J)=AIMAG(ERR(J))
IF (J-2) 5,6,10
5 FREQZ=FG+DF
S(2)=CMPLX(ALFG,FREQZ)
GO TO 10
6 ALFAZ=ALFG+DA
S(3)=CMPLX(ALFAZ,FG)
FREQZ=FG
10 CONTINUE
DERDF=(ER(2)-ER(1))/DF
DERDA=(ER(3)-ER(1))/DA

```

```

DEIDF=(EI(2)-EI(1))/DF
DEIDA=(EI(3)-EI(1))/DA
ALFAZ=ALFG-(EI(1)/DEIDF-ER(1)/DERDF)/(DEIDA/DEIDF-DERDA/DERDF)
FREQZ=FG-(EI(1)/DEIDA-ER(1)/DERDA)/(DEIDF/DEIDA-DERDF/DERDA)
SZ=CMPLX(ALFAZ,FREQZ)
IF(L-30)15,17,17
17 WRITE(6,173) L,SZ,S(1),SS
WRITE(6,170) ERR(J),ESAVE2,ESAVE1
GO TO 55
15 IF(ABS((ALFG-ALFAZ)/ALFAZ).GT..02.OR.ABS(ALFG-ALFAZ)
*.GT.1.) GO TO 9
IF(ABS((FG-FREQZ)/(FG*MACH)).LE..05) GO TO 45
9 FG=FREQZ
ALFG=ALFAZ
ESAVE2=ERR(J)
IF(L.EQ.28)ESAVE1=ERR(J)
SS=S(1)
S(1)=CMPLX(ALFAZ,FREQZ)
L=L+1
GO TO 1
45 IF(IFLAGO.EQ.1) GO TO 46
CALL NBS(IOX,ROX,COX,TAUOX,SZ,NBOX,VCTROX,THETAO)
46 IF(IFLAGF.EQ.1) GO TO 47
CALL NBS(IFU,RFU,CFU,TAUF,SZ,NBF,VCTRF,THETA F)
47 CALL NCS(SZ,NC(J))
GO TO 51
50 SZ=S(J)
51 CSROX=1./(COX*SZ)
CSR F=1./(CFU*SZ)
ISOX=IOX*SZ
ISF=IFU*SZ
TAUSOX=-TAUOX*SZ
TAUSF=-TAUF*SZ
TSROX=REAL(TAUSOX)
TSRF=REAL(TAUSF)
XTSROX=EXP(TSROX)
XTSRF=EXP(TSRF)
TSIOX=AIMAG(TAUSOX)
TSIF=AIMAG(TAUSF)
SZI=AIMAG(SZ)
HZ=SZI/(2.*PI)
WOWO=HZ/FREQN
GROW=REAL(SZ)
SZHZ=CMPLX(GROW,HZ)
AOW=GROW/HZ
IF(L.GE.30)SZ=SSAVE
IF(I.EQ.1)SSAVE=SZ
52 WRITE(6,159)
WRITE(6,160)WOX,PDOX,DELPOX,ROX,COX,CSROX,DPOPCO
WRITE(6,161)WF,PDF,DELPF,RFU,CFU,CSR F,DPOPCF
WRITE(6,162)
IF(IFLAGO.NE.1) GO TO 63

```



```

168  FORMAT(1H ,7HOXIDANT,2X,9G12.4)
169  FORMAT(1H ,4HFUEL,5X,9G12.4)
170  FORMAT(1H ,42HERROR IN RESPONSE FUNCTIONS ARE FOR L=30 ,2F9.4,
*6H L=29 ,2F9.4,9X,6H L=28 ,2F9.4)
171  FORMAT(1H0,43HUNITS USED ARE LB-FT-SEC-DEG R UNLESS NOTED)
172  FORMAT(1H0/1H0/1H0/1H0)
173  FORMAT(1H ,30HABS(ERROR) DIVERGES. ITERATION=,I2,10H CALC'D S=,
*2F9.2,6H S(1)=,2F9.2,15H PREVIOUS S(1)=,2F9.2)
174  FORMAT(4G12.6,3I2)
175  FORMAT(2F12.6,I12)
499  FORMAT(2F20.10,2I2)
708  FORMAT (2I10)
709  FORMAT (6E12.5)
710  FORMAT(1H0,1X,5HDEL X,8X,4HPMAX,8X,4HPMIN,6X,5HWHICH,8X,2HNP,
*9X,3HMAP)
720  FORMAT(1H ,26HOXIDANT IS CHOKED, PCHOKE=,F12.5,5X,
*15HDELP CHOKED/PC=,F12.5)
721  FORMAT(1H ,23HFUEL IS CHOKED, PCHOKE=,F12.5,8X,
*15HDELP CHOKED/PC=,F12.5)
730  FORMAT(1H0,1X,21HINITIAL (GROWTH,FREQ),2X,6HINPUTF)
STOP
END
$IBFTC WO
SUBROUTINE WOP(GC,C,W,A,T,V,D,AC,AR,AI,RHOD,DELP,IFLAG,PCHOKE)
COMMON /AMAIN/PI,GCON,GASC,PC,WTOT
DIMENSION PDKNO(5),WKO(5),TERM1(5),TERM2(5)
G=GC
IFLAG=0
GP=(G+1.)/G
GTW=2./G
GM=(G-1.)/G
GMR= 1./GM
GR=1./G
TOM=T
PCHOKE=PC/((2./(G+1.))**GMR)
TERMO=(PC/PCHOKE)**GTW
TERMT=(PC/PCHOKE)**GP
PCGM=PC**GM
PCGR=PC**GR
WCHOKE=A*C*PCHOKE*SQRT(2.*GCON*GMR*(TERMO-TERMT)/(GASC*TOM))
IF((W-WCHOKE).GT.0.) GO TO 50
DPD=(PCHOKE-PC)/4.
PDKNO(1)=PCHOKE
PDKNO(2)=PCHOKE-DPD
PDKNO(3)=PDKNO(2)-DPD
PDKNO(4)= PDKNO(3)-DPD
PDKNO(5)= PC
WKO(1)=WCHOKE
WKO(5)=0.
DO 10 I=2,4
TERM1(I)=(PC/PDKNO(I))**GTW
TERM2(I)=(PC/PDKNO(I))**GP

```

```

WKO(I)=A*C*PDKNO(I)*SQRT(2.*GCON*GMR*(TERM1(I)-TERM2(I)))/
*(GASC*TOM)
10  CONTINUE
    ONE=(W-WKO(2))*(W-WKO(3))*(W-WKO(4))*(W-WKO(5))/
    *( (WKO(1)-WKO(2))*(WKO(1)-WKO(3))*(WKO(1)-WKO(4))*(WKO(1)-WKO(5)))
    TWO=(W-WKO(1))*(W-WKO(3))*(W-WKO(4))*(W-WKO(5))/
    *( (WKO(2)-WKO(1))*(WKO(2)-WKO(3))*(WKO(2)-WKO(4))*(WKO(2)-WKO(5)))
    THR=(W-WKO(1))*(W-WKO(2))*(W-WKO(4))*(W-WKO(5))/
    *( (WKO(3)-WKO(1))*(WKO(3)-WKO(2))*(WKO(3)-WKO(4))*(WKO(3)-WKO(5)))
    FOR=(W-WKO(1))*(W-WKO(2))*(W-WKO(3))*(W-WKO(5))/
    *( (WKO(4)-WKO(1))*(WKO(4)-WKO(2))*(WKO(4)-WKO(3))*(WKO(4)-WKO(5)))
    FIV=(W-WKO(1))*(W-WKO(2))*(W-WKO(3))*(W-WKO(4))/
    *( (WKO(5)-WKO(1))*(WKO(5)-WKO(2))*(WKO(5)-WKO(3))*(WKO(5)-WKO(4)))
    PD=PDKNO(1)*ONE+PDKNO(2)*TWO+PDKNO(3)*THR+PDKNO(4)*FOR+PDKNO(5)*
    *FIV
20  RHOD=PD/(GASC*TOM)
    DELP=PD-PC
    GMM=(1.-G)/G
    PCGMM=PC**GMM
    PDGMM=PD**GMM
    PDGM=PD**GM
    ALPHA=1./G+GM/2.*1./(1.-PCGMM*PDGM)
    BETA=GM/2.*1./(1.-PCGM*PDGMM)
    AR=-1./ALPHA
    AI=W*D/(GCON*PC*A)
    AC=RHOD*V/(BETA*G*W)
    AC=-AC*ALPHA
    GO TO 60
50  TERMTH=SQRT(GMR*(TERMO-TERMT)*2.*GCON/(GASC*TOM))
    PD=W/(A*C*TERMTH)
    IFLAG=1
    DELP=PD-PC
60  RETURN
    END
$IBFTC NB
    SUBROUTINE NBS(AI,AR,AC,TAU,S,NB,VECT,THET)
    COMPLEX S,EXPO,NB,NOTAU
    EXPO=CEXP(-TAU*S)
    NOTAU=-AC*S/(1.+AC*AR*S+AC*AI*S*S)
    NB=NOTAU*EXPO
    VECT=CABS(NOTAU)
    THET=ATAN2(AIMAG(NOTAU),REAL(NOTAU))*180./3.1416
    RETURN
    END
$IBFTC CH
    SUBROUTINE CHMBR(XA,CA,GA,A)
    COMMON /BF/F
    DIMENSION F(200),B(50,4),T(3),U(3,3),V(3)
    EQUIVALENCE(F(1),B(1,1))
    X=XA
    I=0
10  I=I+1

```

```

      IF (B(I,1).LT.X) GO TO 10
      T(2)= B(I,1)
      U(2,1)= B(I,2)
      U(2,2)= B(I,3)
      U(2,3)= B(I,4)
      I= I+1
      T(3)= B(I,1)
      U(3,1)= B(I,2)
      U(3,2)= B(I,3)
      U(3,3)= B(I,4)
      I= I-2
      T(1)= B(I,1)
      U(1,1)= B(I,2)
      U(1,2)= B(I,3)
      U(1,3)= B(I,4)
      ZERO=(X-T(2)) * (X-T(3)) / ((T(1)-T(2)) * (T(1)-T(3)))
      ONE = (X-T(1)) * (X-T(3)) / ((T(2)-T(1)) * (T(2)-T(3)))
      TWO = (X-T(1)) * (X-T(2)) / ((T(3)-T(1)) * (T(3)-T(2)))
      DO 20 M=1,3
      V(M)= U(1,M)*ZERO+U(2,M)*ONE+U(3,M)*TWO
20    CONTINUE
      CA= V(1)
      GA= V(2)
      A= V(3)
      RETURN
      END
$IBFTC NS
      SUBROUTINE NCS(S,NC)
      COMPLEX EXPT,EXPO,NC,BRAKO,BRAKT
      COMPLEX S,GN,SQR,XONE,XTWO,D,C,E,XONEL,XTWOL
      REAL LL
      COMMON /SCLL/VZ,AMOR,AMV,GC,VV,LL,AA,GNR,GNI
      GN=CMPLX(GNR,GNI)
      SQR=CSQRT((VZ*S*VZ*S)+(S*S+AMOR)*AMV)
      XONE= (VZ*S+SQR)/AMV
      XTWO= (VZ*S-SQR)/AMV
      D= AMV+GC*GN*VV
      E= (GC*GN-1.)*VZ*S
      C=- (XONE*D+E)/(XTWO*D+E)
      XONEL=-XONE*LL
      XTWOL=-XTWO*LL
      EXPO=CEXP(XONEL)
      EXPT=CEXP(XTWOL)
      BRAKO=XONE*EXPO+XTWO*C*EXPT
      BRAKT=EXPO+C*EXPT
      NC=1./GC-AA*BRAKO/(GC*VZ*(S*BRAKT+VZ*BRAKO))
      RETURN
      END
$IBFTC BD
      BLOCK DATA
      DIMENSION F(200)
      COMMON /BF/F

```



```

COMMON /AMAIN/PI,GCON,GASC,PC,WTOT
DATA PI,GCON,GASC/3.1416,32.17,1546./
DATA (F(J),J=1,50)/.004,.006,.008,.01042,.010989,.011628,.012346,
A.013158,.014085,.015152,.016396,.017857,.019608,.021739,.024390,
B.027778,.032258,.038462,.047619,.062500,.0666667,.071429,.076923,
C.083333,.090909,.111111,.142857,.200000,.208333,.217391,.227273,
D.238095,.250000,.263158,.277778,.294118,.312500,.333333,.350000,
E.400000,.450000,.500000,.550000,.60,.65,.70,.75,.80,.85,.90/
DATA (F(J),J=51,100)/2210.,
A2516.,2781.,3062.,3124.,3194.,3265.,3345.,3433.,3532.,3641.,3764.,
B3904.,4064.,4249.,4462.,4712.,5008.,5374.,5867.,5991.,6127.,6277.,
C6445.,6634.,7089.,7653.,8216.,8261.,8300.,8335.,8363.,8384.,8397.,
D8402.,8398.,8384.,8358.,8332.,8222.,8077.,7903.,7705.,7491.,7263.,
E7023.,6773.,6511.,6237.,5947./
DATA (F(J),J=101,150)/1.3259,1.3080,1.2958,1.2829,1.2801,
A1.2769,1.2734,1.2694,1.2648,1.2594,1.2529,1.2449,1.2350,1.2227,
B1.2078,1.1907,1.1727,1.1559,1.1421,1.1321,1.1306,1.1292,1.1280,
C1.1270,1.1261,1.1254,1.1331,1.1650,1.1716,1.1791,1.1876,1.1971,
D1.2077,1.2191,1.2312,1.2436,1.2559,1.2681,1.2766,1.2986,1.3177,
E1.3353,1.3517,1.3661,1.3763,1.3842,1.3893,1.3922,1.3943,1.3966/
DATA (F(J),J=151,200)/
A31.136,30.721,30.318,29.844,29.733,29.612,29.476,29.323,29.151,
B28.956,28.731,28.469,28.160,27.789,27.732,26.751,25.984,24.931,
C23.430,21.210,20.642,20.020,19.337,18.585,17.750,15.772,13.225,
D9.946,9.578,9.203,8.823,8.437,8.046,7.651,7.252,6.852,6.450,6.048,
E5.760,5.040,4.480,4.032,3.665,3.360,3.102,2.880,2.688,2.520,2.372,
F2.240/

```

END

\$IBFTC RS

SUBROUTINE RSTRP(I,J)

REAL LL,LOX,LF

DIMENSION V(14)

COMMON/ERM/FRMAX,FIMAX,FRMIN,FIMIN,FRCUT,FICUT,IOX,ROX,COX,

*TAUOX,CFU,RFU,IFU,TAUF,IFLAGO,IFLAGF,WF,WOX

COMMON/WH/ R,AT,TOMOX,TOMF,AOX,AF,LOX,LF,VOX,VF

COMMON /SCLL/VZ,AMOR,AMV,GC, VV,LL,AA,GNR,GNI

IF(I.GT.1) GO TO 5

V(1)=LL

V(2)=R

V(3)=AT

V(4)=TOMOX

V(5)=TOMF

V(6)=AOX

V(7)=AF

V(8)=LOX

V(9)=LF

V(10)=VOX

V(11)=VF

V(12)=TAUOX

V(13)=TAUF

RETURN

5 GO TO (11,12,13,14,15,16,17,18,19,20,21,22,23),J

```

11    LL=V(1)
      RETURN
12    R=V(2)
      RETURN
13    AT=V(3)
      RETURN
14    TOMOX=V(4)
      RETURN
15    TOMF=V(5)
      RETURN
16    AOX=V(6)
      RETURN
17    AF=V(7)
      RETURN
18    LOX=V(8)
      RETURN
19    LF=V(9)
      RETURN
20    VOX=V(10)
      RETURN
21    VF=V(11)
      RETURN
22    TAUOX=V(12)
      RETURN
23    TAUF=V(13)
      RETURN
      END

```

\$IBFTC WHH

```

      SUBROUTINE WHICHP (WHICH, JP, PMAX, DP)
      REAL LL, LOX, LF
      INTEGER WHICH
      COMMON /SCLL/VZ, AMOR, AMV, GC, VV, LL, AA, GNR, GNI
      COMMON/ERM/FRMAX, FIMAX, FRMIN, FIMIN, FRCUT, FICUT, IOX, ROX, COX,
*TAUOX, CFU, RFU, IFU, TAUF, IFLAGO, IFLAGF, WF, WOX
      COMMON/WH/ R, AT, TOMOX, TOMF, AOX, AF, LOX, LF, VOX, VF
      GO TO (410, 411, 412, 413, 414, 415, 416, 417, 418, 419, 420, 421,
*422), WHICH
410   IF (JP.EQ.1) LL=PMAX+DP
      LL=LL-DP
      WRITE (6, 480) LL
      GO TO 400
411   IF (JP.EQ.1) R =PMAX+DP
      R=R-DP
      WRITE (6, 481) R
      GO TO 400
412   IF (JP.EQ.1) AT =PMAX+DP
      AT=AT-DP
      WRITE (6, 482) AT
      GO TO 400
413   IF (JP.EQ.1) TOMOX=PMAX+DP
      TOMOX=TOMOX-DP
      WRITE (6, 483) TOMOX

```

```

GO TO 400
414 IF (JP.EQ.1) TOMF =PMAX+DP
TOMF=TOMF-DP
WRITE (6,484) TOMF
GO TO 400
415 IF (JP.EQ.1) AOX =PMAX+DP
AOX=AOX-DP
WRITE (6,485) AOX
GO TO 400
416 IF (JP.EQ.1) AF =PMAX+DP
AF=AF-DP
WRITE (6,486) AF
GO TO 400
417 IF (JP.EQ.1) LOX =PMAX+DP
LOX=LOX-DP
WRITE (6,487) LOX
GO TO 400
418 IF (JP.EQ.1) LF =PMAX+DP
LF=LF-DP
WRITE (6,488) LF
GO TO 400
419 IF (JP.EQ.1) VOX =PMAX+DP
VOX=VOX-DP
WRITE (6,489) VOX
GO TO 400
420 IF (JP.EQ.1) VF =PMAX+DP
VF=VF-DP
WRITE (6,490) VF
GO TO 400
421 IF (JP.EQ.1) TAUOX=PMAX+DP
TAUOX=TAUOX-DP
WRITE (6,491) TAUOX
GO TO 400
422 IF (JP.EQ.1) TAUF =PMAX+DP
TAUF=TAUF-DP
WRITE (6,492) TAUF
480 FORMAT (1H ,15HCHAMBER LENGTH=, 5X,G11.5)
481 FORMAT (1H ,15HCHAMBER RADIUS=, 5X,G11.5)
482 FORMAT (1H ,19HNOZZLE THROAT AREA=, 5X,G11.5)
483 FORMAT (1H ,20HOXIDANT TEMP/MOL WT=, 5X,G11.5)
484 FORMAT (1H ,20HFUEL TEMP/MOL WT=, 5X,G11.5)
485 FORMAT (1H ,21HOXIDANT ORIFICE AREA=, 5X,G11.5)
486 FORMAT (1H ,18HFUEL ORIFICE AREA=, 5X,G11.5)
487 FORMAT (1H ,24HOXIDANT INJECTOR LENGTH=, 5X,G11.5)
488 FORMAT (1H ,21HFUEL INJECTOR LENGTH=, 5X,G11.5)
489 FORMAT (1H ,20HOXIDANT DOME VOLUME=, 5X,G11.5)
490 FORMAT (1H ,17HFUEL DOME VOLUME=, 5X,G11.5)
491 FORMAT (1H ,30HOXIDANT COMBUSTION DELAY TIME=, 5X,G11.5)
492 FORMAT (1H ,27HFUEL COMBUSTION DELAY TIME=, 5X,G11.5)
400 RETURN
END
$IBFTC MP

```

```

SUBROUTINE ERMAP
REAL LL, IOX, IFU
INTEGER FRCUT, FICUT, QUAD(20,40)
COMPLEX S, NB, NC, NBOX, NBF, DRESP
DIMENSION ERR(20,40), TR(20), TI(40)
COMMON /SCLL/VZ, AMOR, AMV, GC, VV, LL, AA, GNR, GNI
COMMON/ERM/FRMAX, FIMAX, FRMIN, FIMIN, FRCUT, FICUT, IOX, ROX, COX,
*TAUOX, CFU, RFU, IFU, TAUF, IFLAGO, IFLAGF, WF, WOX
COMMON /AMAIN/PI, GCON, GASC, PC, WTOT
FR=FRMAX
DFR=0.
DFI=0.
IF (FRCUT.NE.1) DFR=(FRMAX-FRMIN)/FLOAT(FRCUT)
IF (FICUT.NE.1) DFI=(FIMAX-FIMIN)/FLOAT(FICUT)
DO 1000 I=1, FRCUT
FI=FIMAX
DO 1010 J=1, FICUT
S=CMPLX(FR, FI)
IF (IFLAGO.EQ.1) GO TO 40
40 CALL NBS (IOX, ROX, COX, TAUOX, S, NBOX, A, B)
IF (IFLAGF.EQ.1) GO TO 80
80 CALL NBS (IFU, RFU, CFU, TAUF, S, NBF, A, B)
NB=(WOX*NBOX+WF*NBF)/WTOT
CALL NCS (S, NC)
DRESP=NB-NC
ANGLE=ATAN2 (AIMAG (DRESP), REAL (DRESP))
IF (ANGLE) 500, 510, 520
500 IF (ANGLE+PI/2.) 600, 601, 601
510 QUAD (I, J)=0
GO TO 90
520 IF (ANGLE-PI/2.) 605, 605, 606
600 QUAD (I, J)=3
GO TO 90
601 QUAD (I, J)=4
GO TO 90
605 QUAD (I, J)=1
GO TO 90
606 QUAD (I, J)=2
GO TO 90
90 ERR (I, J)=CABS (NB-NC)
FI=FI-DFI
1010 CONTINUE
TR (I)=FR
FR=FR-DFR
1000 CONTINUE
FI=FIMAX
DO 1020 J=1, FICUT
TI (J)=FI
FI=FI-DFI
1020 CONTINUE
WRITE (6, 920)
WRITE (6, 900) (TR (J), J=1, FRCUT)

```

```

WRITE(6,905)
DO 1030 J=1,FICUT
WRITE(6,910) TI(J), (ERR(I,J), QUAD(I,J), I=1, FRCUT)
1030 CONTINUE
WRITE(6,905)
900 FORMAT(1H ,1X,4HFREQ,58X,6HGROWTH/1H ,8X,15F8.1)
905 FORMAT(1H ,128H-----)
*-----)
910 FORMAT(1H ,F6.0,1H-,1X,15(F6.2,1H*,11))
920 FORMAT(1H0,58HMAP OF ERRORS, WHICH IS ABS(NB-NC), AND *QUADRANT OF
* ERROR)
RETURN
END

$DATA
2.658      2.658      1.36      1.      .19514E-02      .27833E-03
.36574E-02  .50255E-04      16.875      1      .5
.505      .3      1.41      1.      .30957E-02      .98092E-02
.24363E-02  .50255E-04      393.      1
.5      .1575      .0185      1.      .9166      0.      1.840.
2.658      .505      .1      .2
.19514E-03      .001      -5.      9900. 6 2 1
750.      -750.      90000.      50000.1540

```

APPENDIX B

PROGRAM INPUT FORMAT

Card 1 6G12.5:

1-12 WMAX maximum oxidant flow rate, lb/sec
13-24 WMIN minimum oxidant flow rate, lb/sec
(= WMAX if no variation in oxidant flow rate)
25-36 GAMOX oxidant specific heat ratio
37-48 CORFOX oxidant injector orifice coefficient
49-60 AOX total oxidant injector area, ft²
61-72 LOX oxidant injector length, ft

Card 2 3G12.5, I12, G12.5:

1-12 VOX total oxidant dome volume, ft³
13-24 TAUOX oxidant combustion delay time, sec
25-36 TOMOX oxidant temperature/molecular weight, °R-mole/lb
37-48 IP number of cases in parametric study
(= 0 or 1 if only one case)
49-60 DELX constant used to increment S (e.g., DELX = 0.5)

Card 3 6G12.5:

1-12 WFMAX maximum fuel flow rate, lb/sec
13-24 WFMIN minimum fuel flow rate, lb/sec
(= WFMAX if no variation in fuel flow rate)
25-36 GAMF fuel specific heat ratio
37-48 CORFF fuel injector orifice coefficient
49-60 AF total fuel injector orifice area, ft²
61-72 LF fuel injector length, ft

Card 4 3G12.5, I12:

1-12 VF total fuel dome volume, ft³
13-24 TAUF fuel combustion delay time, sec
25-36 TOMF fuel temperature/molecular weight, °R-mole/lb
37-48 MAP = 1 if error map desired
= 0 if no error map

Card 5 7F10.5, F2.0:

1-10 LL combustion chamber length, ft
11-20 R chamber radius, ft
21-30 AT nozzle throat area, ft²
31-40 CSTREF C* efficiency
41-50 GNR real part of nozzle admittance
51-60 GNI imaginary part of nozzle admittance
61-70 SM transverse wave mode
71-72 SL longitudinal wave mode

Card 6 4G12.6:

1-12 WOSTD standard oxidant flow rate, lb/sec
(WOSTD = WMAX if no variation in oxidant rate)
13-24 WFSTD standard fuel flow rate, lb/sec
(WFSTD = WFMAX if no variation in fuel rate)
25-36 DW increment in oxidant rate, lb/sec
37-48 DWF increment in fuel rate, lb/sec

Card 7 (If IP = 0) 2G12.6, I12:

1-12 FRINP } initial guess of frequency (FRINP + iFIINP);
13-24 FIINP } dimensions are 1/sec and Hz, respectively
25-36 INPUTF if = 0 ignore above and uses natural frequency
if = 1 use above guessed frequency

Card 7 and on (If IP ≠ 0) 4G12.6, 3I2, Number of cards I = IP:

1-12 Z1(I) parameter maximum value
13-24 Z2(I) parameter minimum value
25-36 Z3(I) } equivalent to FRINP and FIINP;
37-48 Z4(I) } units are 1/sec and Hz, respectively
49-50 IZ1(I) = 0 to 14 (see note (1))
51-52 IZ2(I) number of increments between Z1(I) and Z2(I)
53-54 IZ3(I) equivalent to INPUTF

Last card (If MAP = 1) 4G12.6, 2I2:

1-12 FRMAX
13-24 FRMIN } specify range of complex frequency values
25-36 FIMAX } for error map; units are 1/sec and rad/sec
37-48 FIMIN
49-50 FRCUT number of increments between FRMAX and FRMIN
with maximum = 15
51-52 FICUT number of increments between FIMAX and FIMIN
with maximum = 40

Note (1) - Parameter codes IZ1(I) are assigned as follows:

IZ1(I) Parameter

1	LL	chamber length
2	R	chamber radius
3	AT	nozzle area
4	TOMOX	oxidant temperature/molecular weight
5	TOMF	fuel temperature/molecular weight
6	AOX	oxidant injector area
7	AF	fuel injector area
8	LOX	oxidant injector length
9	LF	fuel injector length
10	VOX	oxidant dome volume
11	VF	fuel dome volume
12	TAUDX	oxidant combustion delay time
13	TAUF	fuel combustion delay time

APPENDIX C

SAMPLE PROBLEM

Input

Card	Columns					
	1 to 12	13 to 24	25 to 36	37 to 48	49 to 60	61 to 72
1	2.658	2.658	1.36	1.	0.19514E-02	0.27833E-03
2	.36574E-02	.50255E-04	16.875	1	.5	-----
3	.505	.3	1.41	1.	.30957E-02	.98092E-02
4	.24363E-02	.50255E-04	393.	1	-----	-----

Card	Columns							
	1 to 10	11 to 20	21 to 30	31 to 40	41 to 50	51 to 60	61 to 70	71 & 72
5	0.5	0.1575	0.0185	1.	0.9166	0.0	1.84	0.

Card	Columns							
	1 to 12	13 to 24	25 to 36	37 to 48	49	51	53	
					&	&	&	
					50	52	54	
6	2.658	0.505	0.1	0.2				
7	.19514E-03	.001	-5.	9900.	6	2	1	
8	750.	-750.	90000.	50000.	15	40		

Sample Calculation

GAS-GAS STABILITY MODEL

UNITS USED ARE LB-FT-SEC-DEG R UNLESS NOTED

INPUT PARAMETER FOR OXIDANT
 W MAX 2.65800
 W MIN 1.36000
 GAMMA 1.00000

INPUT PARAMETER FOR FUEL
 W MAX 0.50500
 W MIN 0.30000
 GAMMA 1.41000

CHAMBER PARAMETERS
 LENGTH 0.50000
 RADIUS 0.15750
 THRDT A 0.18500E-01
 C* EFF 1.00000

DEL X 0.50000
 PMAX 0.19514E-03
 PMIN 0.10000E-02
 WHICH 6

INITIAL (GROWTH,FREQ) INPUT
 -5.00000 9900.00 1

DDME VOL 0.36574E-02
 T/MW 0.10000
 DW 0.10000
 W STD 2.65800

DDME V3L 0.24363E-02
 T/MM 0.393000
 DW 0.20000
 W STD 3.53500

NOZZLE RESPONSE 3
 IP 1

OXIDANT ORIFICE AREA= 0.19514E-03

MAP OF ERRORS, WHICH IS ABS(INB-NC), AND *QUADRANT OF ERROR

FREQ	GROWTH														
	750.0	650.0	550.0	450.0	350.0	250.0	150.0	50.0	-50.0	-150.0	-250.0	-350.0	-450.0	-550.0	-650.0
90000.0	1.36*3	1.30*3	1.25*3	1.19*3	1.14*3	1.08*3	1.03*3	0.97*3	0.92*3	0.85*3	0.81*3	0.75*3	0.70*3	0.65*3	0.61*3
89000.0	1.36*2	1.30*2	1.25*2	1.19*2	1.14*2	1.08*2	1.03*2	0.97*2	0.91*2	0.85*2	0.80*2	0.75*2	0.69*2	0.64*2	0.59*2
88000.0	1.62*2	1.57*2	1.52*2	1.48*2	1.43*2	1.39*2	1.34*2	1.30*2	1.26*2	1.22*2	1.18*2	1.14*2	1.10*2	1.07*2	1.04*2
87000.0	2.07*2	2.03*2	2.00*2	1.96*2	1.93*2	1.89*2	1.85*2	1.83*2	1.80*2	1.77*2	1.74*2	1.72*2	1.69*2	1.67*2	1.65*2
86000.0	2.68*2	2.65*2	2.63*2	2.60*2	2.58*2	2.55*2	2.53*2	2.50*2	2.48*2	2.46*2	2.44*2	2.42*2	2.40*2	2.39*2	2.37*2
85000.0	3.45*2	3.43*2	3.42*2	3.40*2	3.39*2	3.37*2	3.36*2	3.34*2	3.33*2	3.31*2	3.30*2	3.29*2	3.27*2	3.26*2	3.25*2
84000.0	4.43*2	4.43*2	4.43*2	4.43*2	4.43*2	4.42*2	4.42*2	4.42*2	4.41*2	4.41*2	4.40*2	4.40*2	4.39*2	4.39*2	4.38*2
83000.0	5.74*2	5.76*2	5.79*2	5.81*2	5.83*2	5.85*2	5.87*2	5.89*2	5.90*2	5.92*2	5.93*2	5.94*2	5.94*2	5.95*2	5.95*2
82000.0	7.55*2	7.64*2	7.72*2	7.80*2	7.88*2	7.96*2	8.04*2	8.10*2	8.17*2	8.23*2	8.28*2	8.33*2	8.37*2	8.41*2	8.43*2
81000.0	10.14*2	10.38*2	10.63*2	10.88*2	11.13*2	11.39*2	11.66*2	11.89*2	12.13*2	12.37*2	12.59*2	12.79*2	12.97*2	13.13*2	13.28*2
80000.0	13.35*2	13.95*2	14.60*2	15.32*2	16.10*2	16.95*2	17.88*2	18.89*2	19.99*2	21.15*2	22.41*2	23.72*2	25.05*2	25.34*2	27.58*2
79000.0	14.61*3	15.44*3	16.38*3	17.45*3	18.68*3	20.11*3	21.78*3	23.77*3	26.17*3	29.11*3	32.80*3	37.56*3	43.90*3	52.70*3	65.52*3
78000.0	11.89*3	12.34*3	12.83*3	13.34*3	13.88*3	14.45*3	15.05*3	15.69*3	16.35*3	17.02*3	17.70*3	18.36*3	19.00*3	19.59*3	20.13*3
77000.0	8.58*3	8.75*3	8.91*3	9.08*3	9.25*3	9.42*3	9.59*3	9.75*3	9.90*3	10.05*3	10.19*3	10.31*3	10.43*3	10.53*3	10.61*3
76300.0	6.18*3	6.24*3	6.30*3	6.35*3	6.41*3	6.46*3	6.51*3	6.56*3	6.61*3	6.65*3	6.69*3	6.72*3	6.76*3	6.78*3	6.81*3
75000.0	4.52*3	4.54*3	4.55*3	4.57*3	4.58*3	4.60*3	4.61*3	4.63*3	4.64*3	4.65*3	4.66*3	4.67*3	4.68*3	4.69*3	4.70*3
74000.0	3.33*3	3.32*3	3.32*3	3.31*3	3.31*3	3.31*3	3.31*3	3.31*3	3.31*3	3.31*3	3.31*3	3.31*3	3.31*3	3.31*3	3.31*3
73000.0	2.42*3	2.40*3	2.39*3	2.37*3	2.36*3	2.35*3	2.34*3	2.33*3	2.32*3	2.31*3	2.30*3	2.30*3	2.29*3	2.29*3	2.29*3
72000.0	1.72*3	1.69*3	1.66*3	1.64*3	1.62*3	1.59*3	1.57*3	1.55*3	1.54*3	1.52*3	1.51*3	1.51*3	1.49*3	1.48*3	1.48*3
71000.0	1.20*3	1.16*3	1.12*3	1.08*3	1.04*3	1.01*3	0.97*3	0.94*3	0.91*3	0.88*3	0.86*3	0.83*3	0.82*3	0.80*3	0.79*3
70000.0	0.91*3	0.86*3	0.81*3	0.76*3	0.71*3	0.65*3	0.60*3	0.55*3	0.49*3	0.44*3	0.39*3	0.34*3	0.29*3	0.24*3	0.20*3
69000.0	0.96*2	0.92*2	0.88*2	0.83*2	0.79*2	0.75*2	0.71*2	0.67*2	0.63*2	0.59*2	0.55*2	0.52*2	0.49*2	0.47*2	0.45*2
68000.0	1.27*2	1.25*2	1.22*2	1.20*2	1.18*2	1.16*2	1.14*2	1.12*2	1.11*2	1.09*2	1.08*2	1.07*2	1.05*2	1.04*2	1.03*2
67000.0	1.69*2	1.68*2	1.68*2	1.68*2	1.68*2	1.68*2	1.68*2	1.68*2	1.68*2	1.68*2	1.68*2	1.68*2	1.68*2	1.68*2	1.68*2
66000.0	2.10*2	2.12*2	2.15*2	2.19*2	2.22*2	2.26*2	2.31*2	2.35*2	2.40*2	2.45*2	2.51*2	2.57*2	2.63*2	2.69*2	2.75*2

65000.0	2.29*2	2.35*2	2.41*2	2.49*2	2.57*2	2.67*2	2.78*2	2.91*2	3.03*2	3.21*2	3.40*2	3.61*2	3.85*2	4.12*2	4.42*2
64000.0	1.93*2	1.96*2	2.01*2	2.06*2	2.12*2	2.20*2	2.29*2	2.40*2	2.54*2	2.71*2	2.91*2	3.16*2	3.46*2	3.84*2	4.32*2
63000.0	1.21*2	1.17*2	1.14*2	1.10*2	1.07*2	1.04*2	1.01*2	0.99*2	0.98*2	0.99*2	1.00*2	1.04*2	1.09*2	1.17*2	1.26*2
62000.0	0.90*2	0.84*2	0.77*2	0.70*2	0.63*2	0.56*2	0.49*2	0.42*2	0.35*2	0.29*2	0.25*2	0.24*2	0.27*2	0.34*2	0.43*2
61000.0	1.18*2	1.15*2	1.12*2	1.09*2	1.07*2	1.05*2	1.03*2	1.01*2	1.00*2	1.03*2	1.00*2	1.01*2	1.02*2	1.04*2	1.07*2
60000.0	1.60*2	1.59*2	1.58*2	1.56*2	1.56*2	1.55*2	1.54*2	1.54*2	1.54*2	1.54*2	1.55*2	1.56*2	1.57*2	1.58*2	1.59*2
59000.0	2.00*2	2.00*2	1.99*2	1.99*2	1.98*2	1.98*2	1.98*2	1.98*2	1.98*2	1.99*2	1.99*2	2.00*2	2.01*2	2.02*2	2.03*2
58000.0	2.37*2	2.37*2	2.36*2	2.36*2	2.36*2	2.36*2	2.36*2	2.36*2	2.36*2	2.37*2	2.37*2	2.38*2	2.39*2	2.40*2	2.41*2
57000.0	2.71*2	2.71*2	2.71*2	2.70*2	2.70*2	2.71*2	2.71*2	2.71*2	2.71*2	2.72*2	2.72*2	2.73*2	2.74*2	2.74*2	2.74*2
56000.0	3.03*2	3.03*2	3.03*2	3.03*2	3.03*2	3.03*2	3.03*2	3.03*2	3.03*2	3.04*2	3.04*2	3.04*2	3.05*2	3.05*2	3.06*2
55000.0	3.33*2	3.33*2	3.33*2	3.33*2	3.33*2	3.33*2	3.33*2	3.33*2	3.33*2	3.34*2	3.34*2	3.34*2	3.35*2	3.35*2	3.36*2
54000.0	3.62*2	3.62*2	3.62*2	3.62*2	3.62*2	3.62*2	3.63*2	3.63*2	3.63*2	3.63*2	3.64*2	3.64*2	3.64*2	3.65*2	3.65*2
53000.0	3.91*2	3.91*2	3.91*2	3.91*2	3.91*2	3.91*2	3.91*2	3.91*2	3.92*2	3.92*2	3.92*2	3.92*2	3.93*2	3.93*2	3.93*2
52000.0	4.19*2	4.19*2	4.19*2	4.19*2	4.19*2	4.19*2	4.19*2	4.19*2	4.19*2	4.20*2	4.20*2	4.20*2	4.21*2	4.21*2	4.21*2
51000.0	4.46*2	4.46*2	4.46*2	4.46*2	4.46*2	4.46*2	4.47*2	4.47*2	4.47*2	4.47*2	4.47*2	4.47*2	4.48*2	4.48*2	4.48*2

OXIDANT	W	PD,PSI	DEL P,PSI	R	C	RE(I/CS)	IM(I/CS)	DEL P/PC
FUEL	0.5050	3973.663	3683.4005000000000000	1.0000	0.2083E-03	-0.8446E-07	-0.1607E-04	12.6898625
		332.411	42.148	0.3441				0.1452058
OXIDANT IS CHOKED, PCHOKE= 78110.37012								
FUEL	0.1190E-05	-0.3893E-03	0.7406E-01	1.0166	-3.1275	2.9604	0.5833E-01	2.9129
								-179.49
CHAMBER	PC,PSI	C*	SOUND SPD	MACH	D/F	RE(RESPI)	IM(RESPI)	ITERATIONS
	290.263	7864.6	5346.0	0.1415	5.2634	0.4675	0.9202E-02	3

GROWTH RATE= -327.0963 FREQUENCY(HZ)= 9904.554 NATURAL FREQUENCY(HZ)= 9939.918 W/ND= 0.99644 A/W= -0.033025

OXIDANT	W	PD,PSI	DEL P,PSI	R	C	RE(I/CS)	IM(I/CS)	DEL P/PC
FUEL	0.5050	3973.663	373.6245000000000000	1.0000	0.3021E-03	-0.1205E-06	-0.1640E-04	15.6235017
		257.634	18.595	0.1697				0.0777912
OXIDANT IS CHOKED, PCHOKE= 64325.81152								
FUEL	0.8728E-06	-0.3908E-03	0.5321E-01	1.0228	-3.0638	6.0333	0.5096	5.9201
								-179.63
CHAMBER	PC,PSI	C*	SOUND SPD	MACH	D/F	RE(RESPI)	IM(RESPI)	ITERATIONS
	239.039	6913.9	4646.6	0.1418	8.7148	0.6237	0.5366E-01	3

GROWTH RATE= -447.7288 FREQUENCY(HZ)= 9702.728 NATURAL FREQUENCY(HZ)= 8539.489 W/ND= 1.12307 A/W= -0.066145

OXIDANT	W	PD,PSI	DEL P,PSI	R	C	RE(I/CS)	IM(I/CS)	DEL P/PC
FUEL	0.5050	775.421	485.1575000000000000	1.0000	0.2083E-03	-0.8336E-07	-0.1607E-04	1.6714398
		332.411	42.148	0.3441				0.1452058
OXIDANT IS CHOKED, PCHOKE= 78110.37012								
FUEL	0.1190E-05	-0.3856E-03	0.7406E-01	1.0164	-3.1277	2.9599	0.5771E-01	2.9129
								-179.49
CHAMBER	PC,PSI	C*	SOUND SPD	MACH	D/F	RE(RESPI)	IM(RESPI)	ITERATIONS
	290.263	7864.6	5346.0	0.1415	5.2634	0.4723	0.1060E-01	4

GROWTH RATE= -324.0276 FREQUENCY(HZ)= 9905.127 NATURAL FREQUENCY(HZ)= 9939.918 W/ND= 0.99650 A/W= -0.032713

```

OXIDANT  W      PD*PSI  DEL P*PSI  R      C      RE(I/CS)  IM(I/CS)  DELP/PC
          2.6580  775.421  536.3825  0.0000  1.0000  -0.1200E-06  -0.1640E-04  2.2439102
          0.3050  257.634  18.595  0.1697  0.3021E-03  -0.3973E-03  -0.5429E-01  0.0777912

OXIDANT IS CHOKED, PCHOKE= 64325.81152  IM(-TAU*S)  IM(-TAU*S)  VCTOR, T=0  THETA, T=0
FUEL      0.8728E-06  -0.3694E-03  0.5321E-01  1.0227  -3.0639  6.0329  0.5086  5.9200  -179.63

CHAMBER  PC*PSI  C*      SOUND SPD  MACH  D/F      RE(RESPI)  IM(RESPI)  ITERATIONS
          239.039  6913.9  4646.6  0.1418  8.7148  0.6247  0.5544E-01  3

```

GROWTH RATE= -446.2127 FREQUENCY(HZ)= 9703.147 NATURAL FREQUENCY(HZ)= 8439.489 W/HO= 1.12312 A/W= -0.065986

REFERENCES

1. Gregory, John W. ; and Herr, Paul N. : Hydrogen-Oxygen Space Shuttle ACPS Thruster Technology Review. NASA TM X-68146, 1972.
2. Kelly, P. J. ; and Schweickert, T. F. : Space Shuttle Auxiliary Propulsion System Design Study - Final Report. Rept. No. MSC 04423.1, McDonnell Douglas Corp. (NASA contract No. NAS9-12012), Dec. 1972.
3. Chandler, Keith B. : The Main Engine for the Space Shuttle. Seventh JANNAF Combustion Meeting. CPIA Publ. No. 204, vol. 1, Johns Hopkins Univ. , Feb. 1971, pp. 821-834.
4. Crocco, Luigi; and Cheng, Sin-I. : Theory of Combustion Instability in Liquid Propellant Rocket Motors. AGARDograph 8, Butterworth Sci. Pub. , 1956.
5. Reardon, F. H. : Correlation of Sensitive-Time-Lag-Theory Combustion Parameters with Thrust Chamber Design and Operating Variables. Fifth ICRPG Combustion Conference. CPIA Pub. no. 183, Johns Hopkins Univ. , Dec. 1968, pp. 237-244.
6. Feiler, Charles E. ; and Heidmann, Marcus F. : Dynamic Response of Gaseous-Hydrogen Flow System and Its Application to High-Frequency Combustion Instability. NASA TN D-4040, 1967.
7. Priem, Richard J. ; and Guentert, Donald C. : Combustion Instability Limits Determined by a Nonlinear Theory and a One-Dimensional Model. NASA TN D-1409, 1962.
8. Hersch, Martin: A Mixing Model for Rocket Engine Combustion. NASA TN D-2881, 1965.
9. Priem, R. J. ; and Rice, E. J. : Combustion Instability with Finite Mach Number Flow and Acoustic Liners. 12th Symposium (International) on Combustion. The Combustion Inst. , 1969, pp. 149-159.

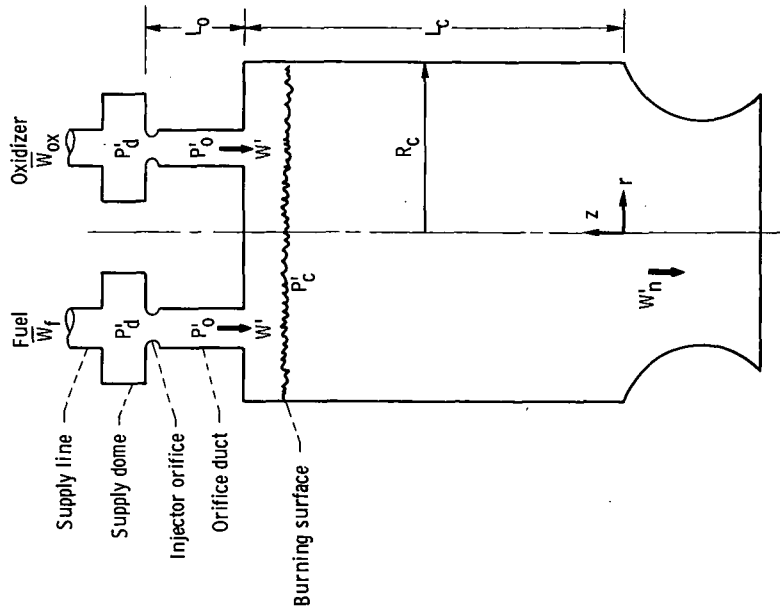


Figure 1. - Schematic of injector and combustion chamber.

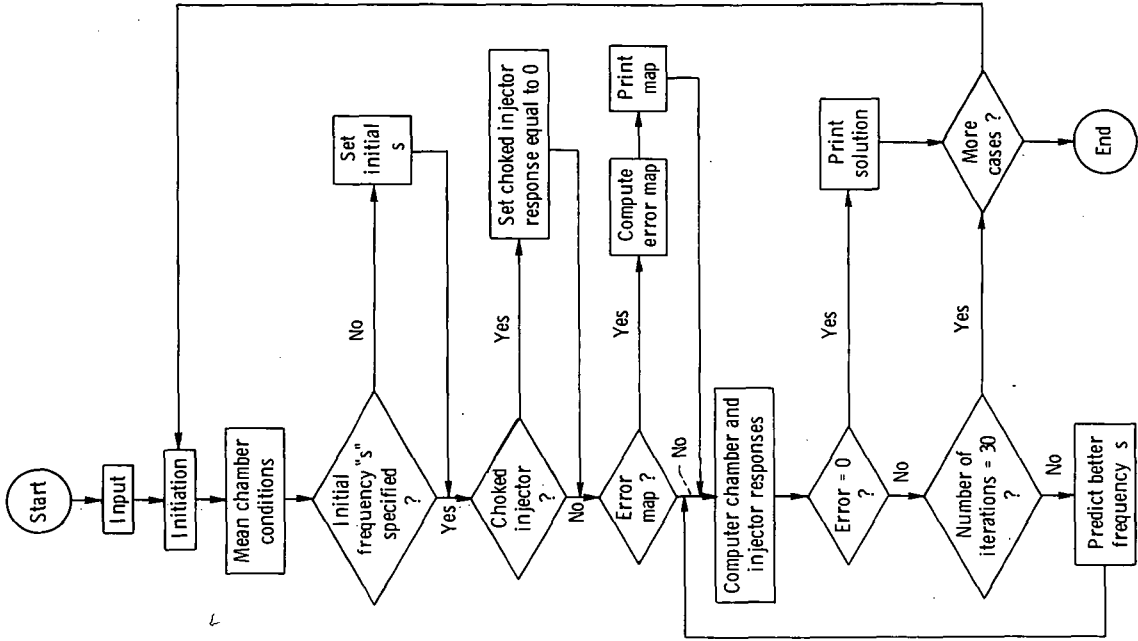
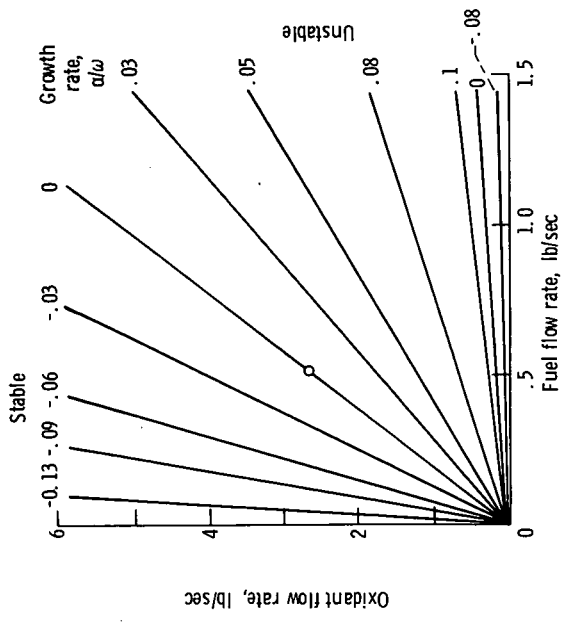
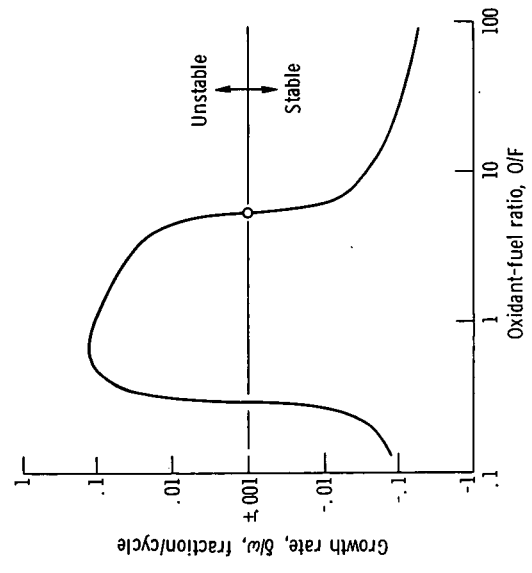


Figure 2. - Computer program flow chart

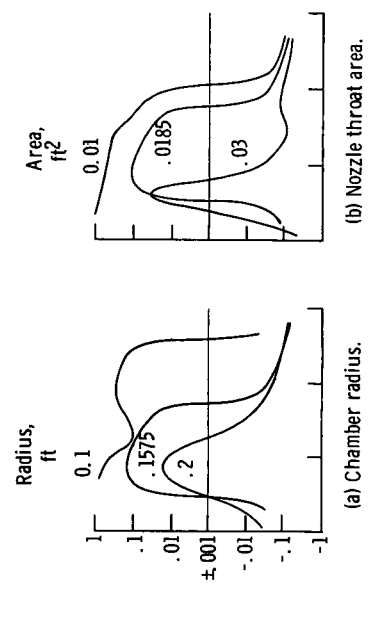


(a) Function of fuel and oxidizer flow rates.

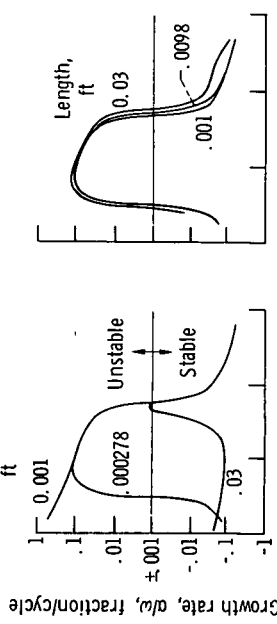


(b) Function of oxidizer to fuel flow ratio.

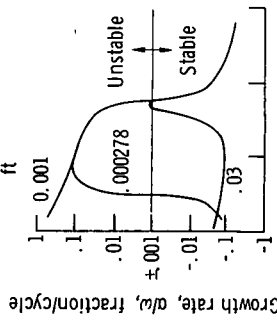
Figure 3. - Stability characteristics of standard engine.



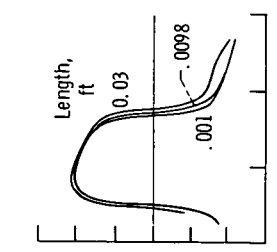
(a) Chamber radius.



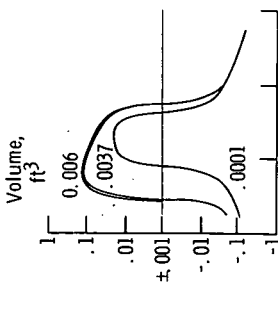
(b) Nozzle throat area.



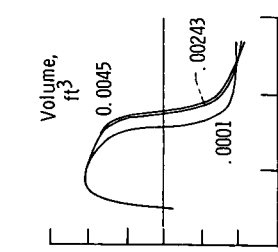
(c) Oxidant injector length.



(d) Fuel injector length.



(e) Oxidant dome volume.



(f) Fuel dome volume.

Figure 4. - Influence of design parameters on stability.

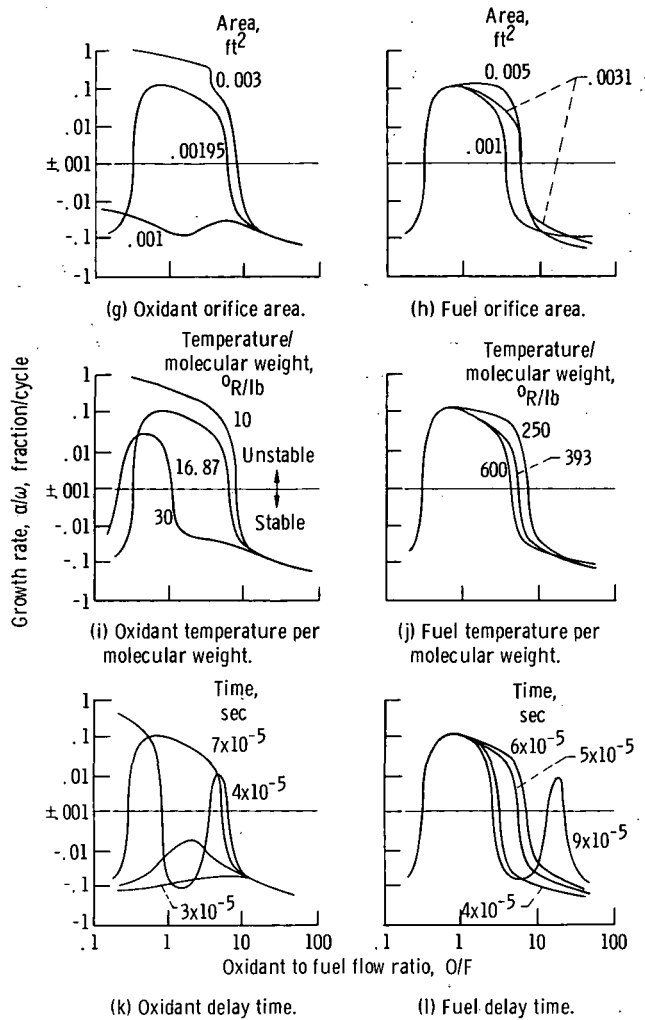


Figure 4. - Concluded.



POSTMASTER: If Undeliverable (Section 158
Postal Manual) Do Not Return

"The aeronautical and space activities of the United States shall be conducted so as to contribute . . . to the expansion of human knowledge of phenomena in the atmosphere and space. The Administration shall provide for the widest practicable and appropriate dissemination of information concerning its activities and the results thereof."

—NATIONAL AERONAUTICS AND SPACE ACT OF 1958

NASA SCIENTIFIC AND TECHNICAL PUBLICATIONS

TECHNICAL REPORTS: Scientific and technical information considered important, complete, and a lasting contribution to existing knowledge.

TECHNICAL NOTES: Information less broad in scope but nevertheless of importance as a contribution to existing knowledge.

TECHNICAL MEMORANDUMS: Information receiving limited distribution because of preliminary data, security classification, or other reasons. Also includes conference proceedings with either limited or unlimited distribution.

CONTRACTOR REPORTS: Scientific and technical information generated under a NASA contract or grant and considered an important contribution to existing knowledge.

TECHNICAL TRANSLATIONS: Information published in a foreign language considered to merit NASA distribution in English.

SPECIAL PUBLICATIONS: Information derived from or of value to NASA activities. Publications include final reports of major projects, monographs, data compilations, handbooks, sourcebooks, and special bibliographies.

TECHNOLOGY UTILIZATION PUBLICATIONS: Information on technology used by NASA that may be of particular interest in commercial and other non-aerospace applications. Publications include Tech Briefs, Technology Utilization Reports and Technology Surveys.

Details on the availability of these publications may be obtained from:

SCIENTIFIC AND TECHNICAL INFORMATION OFFICE

NATIONAL AERONAUTICS AND SPACE ADMINISTRATION

Washington, D.C. 20546